hep-lat 0812.0503

arXiv:0812.0503v3 [hep-lat] 2 Apr 2009

Radiative corrections to the lattice gluon action for highly improved staggered quarks (HISQ) and the effect of such corrections on the static potential

A. Hart,[1] G.M von Hippel,[2] and R.R. Horgan[3]
(HPQCD Collaboration)

[1]*SUPA, School of Physics and Astronomy, University of Edinburgh, Edinburgh EH9 3JZ, United Kingdom*
[2]*Deutsches Elektronen-Synchrotron DESY, 15738 Zeuthen, Germany*
[3]*Department of Applied Mathematics and Theoretical Physics, University of Cambridge, Centre for Mathematical Sciences, Cambridge CB3 0WA, United Kingdom*

We perform a perturbative calculation of the influence of dynamical HISQ fermions on the perturbative improvement of the gluonic action in the same way as we have previously done for asqtad fermions. We find the fermionic contributions to the radiative corrections in the Lüscher-Weisz gauge action to be somewhat larger for HISQ fermions than for asqtad. Using one-loop perturbation theory as a test, we estimate that omission of the fermion-induced radiative corrections in dynamical asqtad simulations will give a measurable effect. The one-loop result gives a systematic shift of about -0.6% in $\hat{r}_1$ on the coarsest asqtad improved staggered ensembles. This is the correct sign and magnitude to explain the scaling violations seen in $\Phi_B = f_B\sqrt{M_B}$ on dynamical lattice ensembles.

PACS numbers: 12.38.Bx, 12.38.Gc, 13.20.Gd

I. INTRODUCTION

The Fermilab, MILC, HPQCD and UKQCD Collaborations are involved in an ambitious programme of high precision predictions of phenomenologically relevant parameters from QCD using unquenched lattice simulations [1].

Central to this programme is the perturbative improvement of the fermionic and gluonic action and operators to remove significant sources of scaling violation in the lattice simulation results. This body of work is based on the Symanzik-improved staggered-quark formalism, specifically the use of the asqtad action [2]. More recently, the Highly Improved Staggered Quark (HISQ) action has been used to further suppress taste-changing interactions and to allow the use of heavier quarks at the same lattice spacing by removing tree-level $\mathcal{O}((ma)^4)$ artifacts from the valence quark action [3].

To maintain the same level of improvement when these actions are used to describe the sea quarks [4, 5], we should include the effect of fermion loops on the radiative terms in the Symanzik–improved gauge action. This has recently been done to $\mathcal{O}(N_f\alpha_s a^2)$ for the asqtad action [6] and in this paper we update that calculation to include dynamical HISQ fermions instead. Some preliminary results can be found in Ref. [7]. We note that the corrections are larger for HISQ than for asqtad.

In the second part of this paper, Sec. IV, we consider what effect the $\mathcal{O}(N_f\alpha_s a^2)$ will have in a practical simulation, particularly on the scale-setting parameters $\hat{r}_1$ and $\hat{r}_0$ derived from the static quark potential.

The MILC and UKQCD Collaborations have already used dynamical asqtad quarks to generate a large set of Monte Carlo lattice ensembles, including ones with very light sea quarks (MILC, e.g. [1]) and ones with large numbers of independent configurations (UKQCD [8]).

The gauge action used, however, omitted the asqtad $\mathcal{O}(N_f\alpha_s a^2)$ radiative improvements (they were not then known). It has been observed that the quantity $\Phi_B = f_B\sqrt{M_B}$ shows a $+2\%$ scaling violation on the dynamical "coarse" ensembles (lattice spacing $a \simeq 0.12$ fm) relative to the "fine" ($a \simeq 0.09$ fm) [9]. This scaling violation was not seen for corresponding quenched lattices [10].

Unless there is a subtle (and therefore unlikely) cancellation, the quenched result suggests that the (quenched) gluonic and valence staggered actions are not the problem. If the asqtad action is suitable for the valence quarks, it seems likely it is equally suitable for the sea quarks. The scaling violation is therefore argued to arise from the omission of the $\mathcal{O}(N_f\alpha_s a^2)$ radiative corrections to the gluonic action. It is certainly plausible that the fermionic contributions could have such an effect; they are, after all, large enough to reverse the sign of some of the radiative couplings in the action [6].

In these calculations $\hat{r}_1 \equiv r_1/a$ has been used to set the scale, i.e. to convert from dimensionless lattice results to physical predictions. We therefore attempt to estimate, at least semi-quantitatively, whether the omission of the asqtad $\mathcal{O}(N_f\alpha_s a^2)$ radiative corrections would have a measurable effect on the static potential and, in particular, on the scale-setting parameters $\hat{r}_1$ and $\hat{r}_0$ used to convert from dimensionless lattice results to physical predictions. We do this using one-loop perturbation theory. We treat such a result as indicative: we do not rule out higher loop and non-perturbative contributions, but argue that if one-loop perturbation theory predicts a measurable result then it is likely to persist when we include other contributions.

Using one-loop perturbation theory, we find that including the fermionic radiative corrections to the gauge action would lead to a 0.65% *decrease* in $\hat{r}_1$ on the coarse ensembles and no change on the fine. The sign and magnitude of these shifts are robust under reasonable varia-

tions in fitting parameters. This would equate to a 0.65% *increase* in a on the coarse ensembles. The quantity Φ_B scales as $a^{-3/2}$, so the $\mathcal{O}(N_f\alpha_s a^2)$ corrections would lead to a 1% *decrease* in Φ_B on the coarse ensembles and no effect on the fine.

This shift is very close to what has been observed and we therefore suggest that the anomalous upward shift in Φ_B is in large part due to the omission of the $\mathcal{O}(N_f\alpha_s a^2)$ radiative corrections to the gluon action. We therefore predict that other observables scaling with a similar negative power of a should exhibit similar scaling violations that ought to become noticeable if these observables are measured to similar accuracy.

II. ON-SHELL IMPROVEMENT

We begin by briefly reviewing how radiative improvement works at $\mathcal{O}(\alpha_s a^2)$.

Starting from the Symanzik tree-level–improved gauge action, the Coulomb self-energy from the 1-loop radiative corrections is (see Section 4 of Ref. [11] and Eq. (44) of Ref. [12]):

$$w(\mathbf{k}) \;\propto\; \mathbf{k}^2 + \alpha_s \left(a_1\mathbf{k}^2 - \beta_0 \mathbf{k}^2 \ln(\mathbf{k}^2) + a_2 \mathbf{k}^{(4)} + a_3 (\mathbf{k}^2)^2 \right) \tag{1}$$

where

$$\mathbf{k}^2 = \sum_{i=1}^{3} k_i^2 \;, \quad \mathbf{k}^{(4)} = \sum_{i=1}^{3} k_i^4 \;. \tag{2}$$

The first two terms in the brackets are absorbed into the scheme definition of α_V (Eq. (46) of Ref. [12]) and do not concern us. The last two terms in the brackets are lattice artifacts and are $\mathcal{O}(\alpha_s a^2)$. It is the goal of radiative improvement to remove these terms.

To improve the gauge theory at $\mathcal{O}(\alpha_s a^2)$ we introduce appropriate radiative counterterms into the gauge action. There are four such dimension-6 counterterms: three gluonic operators (named by Lüscher and Weisz [13] as "planar rectangles", "parallelograms" and "bent rectangles", with coefficients c_1, c_2 and c_3 respectively) plus the static quark operator,

$$c_4 \; a^2 \Psi^\dagger \nabla \cdot \mathbf{E} \Psi \;, \tag{3}$$

which contributes specifically to the static-quark potential.

The action normalisation condition

$$c_0 + 8(c_1 + c_2) + 16 c_3 = 1 \tag{4}$$

ensures we get the correct gauge action in the continuum limit and fixes c_0 (the coefficient of the plaquette), given the other coefficients.

On-shell observables will remain unchanged under field redefinitions using the equations of motion. If we confine our attention to on-shell quantities, we can exploit this to set one of the c_i to zero [37]. The usual choice is to set $c_3 = 0$.

Looking at the terms in Eqn. (1) in more detail, the a_2 term breaks rotational symmetry and its effect on the static-quark potential is given by the Fourier transform

$$\delta V_2(r) \sim \alpha_s a^2 \int_{-\pi}^{\pi} \frac{d^3k}{(2\pi)^3} e^{-\mathbf{k}\cdot\mathbf{r}} \; \frac{\mathbf{k}^{(4)}}{(\mathbf{k}^2)^2} \;. \tag{5}$$

The leading $\mathcal{O}(\alpha_s a^2)$ behaviour is $\sim \alpha_s a^2 / r^3$ with $\mathcal{O}(a^4)$ corrections that break rotational symmetry.

The effect of radiative improvement on the static potential is to set $a_2 = 0$, which therefore also restores rotational invariance of the static potential (at this level) and gives the correct Coulomb coefficient α_V [12].

The a_3 term, in contrast, already preserves rotational invariance:

$$\delta V_3(r) \sim \alpha_s a^2 \int_{-\pi}^{\pi} \frac{d^3k}{(2\pi)^3} e^{-\mathbf{k}\cdot\mathbf{r}} \;+\; \mathcal{O}(a^4). \tag{6}$$

with the leading contribution to the static-quark potential being the 3D Kronecker $\delta_{\mathbf{r},\mathbf{0}}$ (seen by changing variables to $z_i = e^{-k_i r_i}$). This, as Snippe points out [12], does not affect the potential at non-zero $r \equiv |\mathbf{r}|$ and will therefore not contribute to the scale setting parameters $\hat{r}_1$ and $\hat{r}_0$. In general, however, we do need to remove it: as well as the contact term there will be an effect for $r > 0$ at higher order (i.e. at $\mathcal{O}(a^4)$) because the denominator in the Symanzik tree-level Coulomb propagator will not exactly cancel the $\mathbf{k}^2$ from the Feynman rules owing to differences in their definitions.

Both c_3 and c_4 contribute to the a_3 term [11, 14] so, with $c_3 = 0$ fixed as above, we can only remove it by introducing the static quark counterterm into the theory [15, 16], i.e. by choosing an appropriate, and non-zero, value for c_4. This has the effect of introducing staples onto temporal Wilson lines, which must be included in numerical simulations. Similarly, the c_4 contact term will be important in, for instance, the $\Upsilon(2S-1S)$ mass splitting. A contact term gives a contribution proportional to the square of the wavefunction at the origin. This is clearly different for the two states concerned, and will change the mass splitting [38]. We will not, however, consider the contact term in detail in this paper.

A. The calculation

Contact term aside, with $c_3 = 0$ we thus need to determine c_1 and c_2 to complete the on-shell improvement. Given two independent quantities Q_1 and Q_2 with expansions

$$Q_i = \bar{Q}_i + w_i (\mu a)^2 + d_{ij} c_j (\mu a)^2 + \mathcal{O}\left((\mu a)^4\right) \;, \tag{7}$$

in powers of (μa), where μ is some energy scale, we obtain the $\mathcal{O}(a^2)$ matching condition

$$d_{ij} c_j = -w_i \;. \tag{8}$$

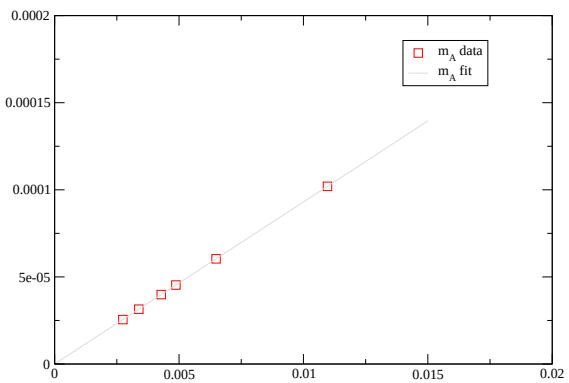

FIG. 1: A plot of the fermionic contributions to the one-loop A meson self-energy $m_A^{(1)}/m$ against $(ma)^2$. The vanishing of $m_A^{(1)}/m$ in the infinite-volume limit can be seen clearly.

Since this equation is linear, both sides can be decomposed into a gluonic and a fermionic part; the gluonic part is known [12, 17] and is independent of the fermion action.

In this paper, we focus on the fermionic contribution to the radiative improvement of the gluon action. Such contributions come from quark loops, which therefore cannot change the tree-level coefficients compared to the quenched case [17]. To compute the one-loop HISQ fermionic corrections to the gluon action, we will follow the same procedure as in the case of the asqtad action [6], using as our two quantities Q_i the three-gluon coupling and the mass of the so-called twisted A meson [13].

B. Lattice perturbation theory

We use lattice perturbation theory to calculate the radiative corrections. The (unsmeared) link variables U_μ are expressed in terms of the gauge field A_μ as

$$U_\mu(x) = \exp\left(gaA_\mu\left(x+\tfrac{1}{2}\hat{\mu}\right)\right) \tag{9}$$

which, when expanded in powers of g, leads to a perturbative expansion of the lattice action, from which the perturbative vertex functions can be derived.

The gauge field A_μ is Lie algebra-valued, and can be decomposed as

$$A_\mu(x) = \sum_a A_\mu^a(x) t^a \ , \tag{10}$$

with the t^a being anti-Hermitian generators of SU(N), where $N = 3$ in the case of QCD.

The improved Lüscher–Weisz action that we study is [18]

$$S = \sum_x \{c_0 P_0(x) + c_1 P_1(x) + c_2 P_2(x)\} \ . \tag{11}$$

with $c_0 + 8(c_1 + c_2) = 1$ and, at tree level, $c_0^{(0)} = \frac{5}{3}$, $c_1^{(0)} = -\frac{1}{12}$, $c_2^{(0)} = 0$. The terms

$$\begin{aligned} P_0 &= \sum_{\mu<\nu} U_{\mu\nu} \ , \\ P_1 &= \sum_{\mu<\nu} \left(U_{\mu\mu\nu} + U_{\mu\nu\nu}\right) \ , \\ P_2 &= \sum_{\mu<\nu<\sigma} \left(U_{\mu\nu\sigma} + U_{\mu\sigma\nu} + U_{\sigma\mu\nu} + U_{\sigma;-\mu;\nu}\right) \ , \end{aligned} \tag{12}$$

are made up of appropriate traced, closed contours of gauge links. The notation here is that μ, ν and σ are summed over positive values and negative subscripts denote hermitian-conjugated gauge links.

The HISQ fermionic action is defined by an iterated smearing procedure with reunitarisation:

$$U^{\mathrm{HISQ}} = (F_{\mathrm{asq}'} \circ P_{U(3)} \circ F_{\mathrm{Fat7}})[U] \tag{13}$$

where $P_{U(3)}$ denotes the polar projection onto $U(3)$ (as used in simulations [5], and *not* $SU(3)$), and the Fat7 and modified asq smearings are defined in Ref. [3].

To handle the complicated form of the vertices and propagators in lattice perturbation theory, we employ a number of automation methods [19, 20, 21, 22, 23, 24] that are based on the seminal work of Lüscher and Weisz [17] and are implemented in the HiPPy package [19, 20].

The multi-level smearing of the gauge fields employed in the HISQ action presents particular problems when deriving the Feynman rules, even when employing automated techniques. The solution to these is discussed in Refs. [7, 20].

Unless otherwise stated, we shall use g^2 as the perturbative expansion parameter (rather than $\alpha_s = \frac{g^2}{4\pi}$), with expansions written in the form:

$$c_i = c_i^{(0)} + g^2 c_i^{(1)} + \mathcal{O}(g^4) \ . \tag{14}$$

The goal of this paper is to determine the fermionic contributions to $c_1^{(1)}$ and $c_2^{(1)}$, with $c_0^{(1)} = -8(c_1^{(1)} + c_2^{(1)})$.

Since we will only consider fermionic loops, we do not need to concern ourselves with the gauge fixing, Haar measure and Fadeev-Popov ghost terms that appear in the gluonic portion of the perturbative Lagrangian.

The loop integrals of continuum perturbation theory are replaced by finite sums over the points of the reciprocal lattice in lattice perturbation theory. We carry out these sums exactly rather than using a stochastic estimator.

C. Twisted boundary conditions

We work on a four-dimensional Euclidean lattice of length La in the x and y directions and lengths $L_z a$, $L_t a$

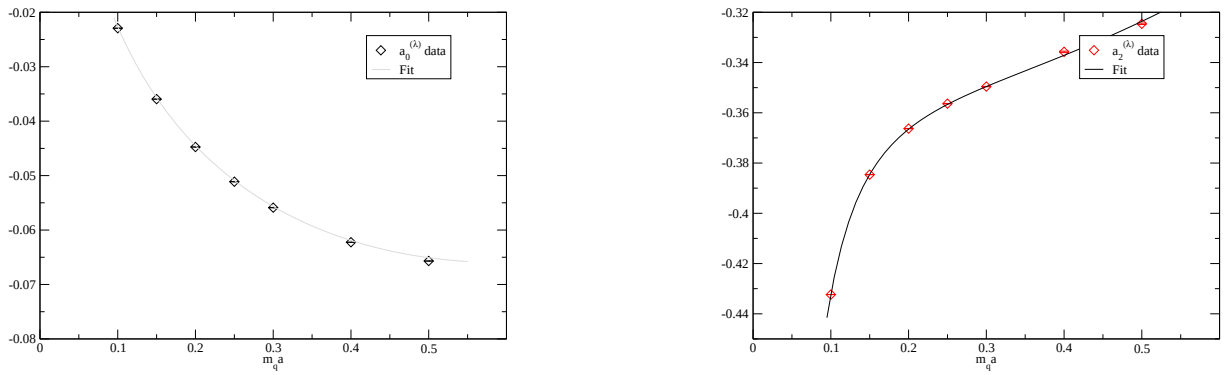

FIG. 2: Plots of $a_0^{(\lambda,1)}$ against $m_q a$ (left) and of $a_2^{(\lambda,1)}$ against $m_q a$ (right) with the fits shown for comparison.

in the z and t directions, respectively, where a is the lattice spacing and L, L_z, L_t are even integers. In the following, we will employ twisted boundary conditions [25] for the same purpose and in essentially the same way as in Refs. [12, 17]. The twisted boundary conditions we use for gluons and quarks are applied to the (x, y) directions and are given by $(\nu = x, y)$

$$\begin{aligned} U_\mu(x + L\hat{\nu}) &= \Omega_\nu U_\mu(x)\Omega_\nu^{-1} \,, \\ \Psi(x + L\hat{\nu}) &= \Omega_\nu \Psi(x)\Omega_\nu^{-1} \,, \end{aligned} \tag{15}$$

where the quark field $\Psi_{sc}(x)$ becomes a matrix in smell-colour space [26] by the introduction of a new SU(N) quantum number "smell" in addition to the quark colour. In the (z, t) directions, we apply periodic boundary conditions.

These boundary conditions lead to a change in the Fourier expansion of the fields:

$$\begin{aligned} A_\mu(x) &= \frac{1}{NL^2L_zL_t} \sum_k \Gamma_k e^{ikx} \tilde{A}_\mu(k) \\ \Psi_\alpha(x) &= \frac{1}{NL^2L_zL_t} \sum_p \Gamma_p e^{ipx} \tilde{\Psi}_\alpha(x) \end{aligned} \tag{16}$$

where the matrices Γ_k are given by (up to an arbitrary phase, which may be chosen for convenience)

$$\Gamma_k = \Omega_1^{-n_2}\Omega_2^{n_1} \tag{17}$$

and in the twisted (x, y) directions the momentum sums are now over

$$p_\nu = mn_\nu, \quad -\frac{NL}{2} < n_\nu \leq \frac{NL}{2}, \quad \nu = (x, y) \,, \tag{18}$$

where $m = \frac{2\pi}{NLa}$. The zero modes ($n_x = n_y = 0 \bmod N$) are omitted from the sum in the case of the gluons, but not the quarks. The momentum sums for quark loops need to be divided by N to remove the redundant smell factor.

We may consider the continuum limit of the twisted theory as a Kaluza-Klein theory in the infinite (z, t) plane. Denoting $\mathbf{n} = (n_x, n_y)$, the stable particles in the (z, t) continuum limit of this effective theory are called the A mesons ($\mathbf{n} = (1, 0)$ or $\mathbf{n} = (0, 1)$) with mass m and the B mesons ($\mathbf{n} = (1, 1)$) with mass $\sqrt{2}m$ [12].

D. Small-mass expansions

Even though we are ultimately interested in the radiative corrections in the chiral limit, we cannot set $m_q a = 0$ straightaway: the correct way to approach the chiral limit is to maintain $m_q/m > C$ as we take $m_q a \to 0$ and $ma \to 0$, where C is a constant determined by the requirement that a Wick rotation can be performed without encountering a pinch singularity [6].

We therefore adopt the following procedure to extract the $\mathcal{O}(a^2)$ lattice artifacts: First, we expand some observable quantity Q in powers of ma at fixed $m_q a$:

$$\begin{aligned} Q(ma, m_q a) = a_0^{(Q)}(m_q a) + a_2^{(Q)}(m_q a)(ma)^2 + \\ \mathcal{O}\left((ma)^4, (ma)^4 \log(ma)\right) \end{aligned} \tag{19}$$

where the coefficients in the expansion are all functions of $m_q a$. There is no term at $\mathcal{O}\left((ma)^2 \log(ma)\right)$ since the gluon action is improved at tree-level to $\mathcal{O}(a^2)$ [12]. Then, we expand the coefficients $a_0^{(Q)}(m_q a)$ in powers of $m_q a$.

For $a_0^{(Q)}(m_q a)$ we have [27]

$$a_0^{(Q)}(m_q a) \;=\; b_{0,0}^{(Q)} \log(m_q a) + a_{0,0}^{(Q)} \,. \tag{20}$$

Since we expect a well-defined continuum limit, $a_0^{(Q)}(m_q a)$ cannot contain any negative powers of $m_q a$, but, depending on the quantity Q, it may contain logarithms; $b_{0,0}^{(Q)}$ is the anomalous dimension associated with Q, and can be determined by a continuum calculation.

There can be no terms in $(m_q a)^{2n}$ for $n > 0$ since there is no counterterm in the gluon action that can compensate for a scaling violation of this kind.

For $a_2^{(Q)}(m_q a)$ we find

$$a_2^{(Q)}(m_q a) = \frac{a_{2,-2}^{(Q)}}{(m_q a)^2} + a_{2,0}^{(Q)} + \left(a_{2,2}^{(Q)} + b_{2,2}^{(Q)} \log(m_q a)\right)(m_q a)^2 + \mathcal{O}\left((m_q a)^4\right) . \quad (21)$$

After multiplication by $(ma)^2$, the $(m_q a)^{-2}$ contribution gives rise to a continuum contribution to Q, and $a_{2,-2}^{(Q)}$ is calculable in continuum perturbation theory. There can be no term in $(m_q a)^{-2}\log(m_q a)$ since this would be a volume-dependent further contribution to the anomalous dimension of Q, and there can be no term in $\log(m_q a)$ since the action is tree-level $\mathcal{O}(a^2)$ improved [28]. A rigorous proof of Eqn. (21) along the lines of Ref. [27] would, of course, be welcome.

In the chiral limit $m_q \to 0$, the term w_i that appears on the right-hand side of Eqn. (8) is $a_{2,0}^{(Q)}$.

E. Twisted spectral quantities

The simplest spectral quantity that can be chosen within the framework of the twisted boundary conditions outlined above is the (renormalised) mass of the A meson. The one-loop correction to the A meson mass is given by [12]

$$m_A^{(1)} = -Z_0(\mathbf{k})\left.\frac{\pi_{11}^{(1)}(k)}{2m_A^{(0)}}\right|_{k=(im_A^{(0)},0,m,0)} \quad (22)$$

where $Z_0(\mathbf{k}) = 1 + \mathcal{O}\left((ma)^4\right)$ is the residue of the pole of the tree-level gluon propagator at spatial momentum $\mathbf{k}$, and $m_A^{(0)}$ is defined so that the momentum k is on-shell.

Gauge invariance implies [6]

$$a_{2,-2}^{(m_A,1)} = 0 ,$$
$$a_0^{(m_A,1)}(m_q a) = 0 . \quad (23)$$

The $\mathcal{O}\left(\alpha_s (ma)^2\right)$ contribution from improvement of the action is given by [12]

$$\Delta_{\text{imp}} \frac{m_A^{(1)}}{m} = -(c_1^{(1)} - c_2^{(1)})(ma)^2 + \mathcal{O}\left((ma)^4\right) , \quad (24)$$

leading to the improvement condition

$$c_1^{(1)} - c_2^{(1)} = a_{2,0}^{(m_A,1)} . \quad (25)$$

The next simplest independent spectral quantity is the scattering amplitude for A mesons at B meson threshold, which can be described by an effective AAB meson coupling constant λ [13]:

$$\lambda = g_0 \sqrt{Z(\mathbf{k})Z(\mathbf{p})Z(\mathbf{q})}\; e_j\, \Gamma^{1,2,j}(k,p,q) \quad (26)$$

where a twist factor of $\frac{i}{N}\text{Tr}([\Gamma_k, \Gamma_p]\Gamma_q)$ has been factored out from from both sides, and the momenta and polarisations of the incoming particles are (with $r > 0$ defined such that $E(\mathbf{q}) = 0$)

$$\begin{array}{ll} k = (iE(\mathbf{k}), \mathbf{k}), & \mathbf{k} = (0, m, ir) \\ p = (-iE(\mathbf{p}), \mathbf{p}), & \mathbf{p} = (m, 0, ir) \\ q = (0, \mathbf{q}), & \mathbf{q} = (-m, -m, -2ir) \\ e = (0, 1, -1, 0) & \end{array} \quad (27)$$

We expand Eqn. (26) perturbatively to one-loop order and find (up to $\mathcal{O}((ma)^4)$ corrections)

$$\frac{\lambda^{(1)}}{m} = \left(1 - \frac{1}{24}m^2\right)\frac{\Gamma^{(1)}}{m} - \frac{4}{k_0}\frac{d}{dk_0}\,\pi_{11}^{(1)}(k)\Big|_{k_0 = iE(\mathbf{k})} - \left(1 - \frac{1}{12}m^2\right)\frac{d^2}{dq_0^2}\left(e^i e^j \pi_{ij}^{(1)}(q)\right)\Big|_{q_0=0} \quad (28)$$

where $\Gamma^{(1)}$ is the one-particle irreducible three-point function at one loop. The derivatives of the Feynman diagrams contributing to the self-energy are computed analytically using automatic differentiation [29, 30]. Continuum calculations of the anomalous dimension and infrared divergence give

$$b_{0,0}^{(\lambda,1)} = -\frac{N_f}{3\pi^2}g^2 ,$$
$$a_{2,-2}^{(\lambda,1)} = -\frac{N_f}{120\pi^2}g^2 . \quad (29)$$

The improvement contribution to λ is [12]

$$\Delta_{\text{imp}} \frac{\lambda^{(1)}}{m} = 4(9c_1^{(1)} - 7c_2^{(1)})(ma)^2 + \mathcal{O}\left((ma)^4\right) , \quad (30)$$

leading to the improvement condition

$$4\left(9c_1^{(1)} - 7c_2^{(1)}\right) = -a_{2,0}^{(\lambda,1)} . \quad (31)$$

III. RESULTS

To extract the improvement coefficients from our diagrammatic calculations, we compute the diagrams for a number of different values of both L and m_q with $N_f = 1$, $N = 3$. At each value of m_q, we then perform a fit in ma of the form given in Eqn. (19) to extract the coefficients $a_n^{(Q,1)}(m_q a)$ for $n = 0, 2$. Our fits confirm that $a_0^{(m_A,1)}(m_q a) = 0$; an example is shown in Fig. 1

Performing a fit of the form in Eqns. (20,21) respectively on these coefficients, we are able to extract the analytically-known coefficients with high accuracy along with the required $(ma)^2$ contributions, as shown in Fig. 2.

Our results for the fermionic contributions are

$$a_{2,0}^{(m_A,1)} = 0.00942(3) ,$$
$$a_{2,0}^{(\lambda,1)} = -0.352(2) . \quad (32)$$

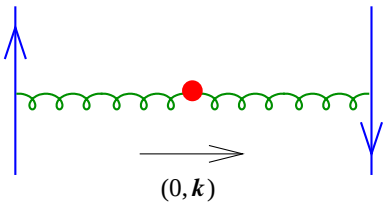

FIG. 3: The one-loop counterterm contribution to the static potential.

Equating these results with the w_i of Eqn. (8), we can solve Eqns. (25,31) for $c_i^{(1)}$ to obtain

$$\begin{aligned} c_1^{(1)} &= -0.025218(4) + 0.0110(3)N_f \\ c_2^{(1)} &= -0.004418(4) + 0.0016(3)N_f \\ \Rightarrow \quad c_0^{(1)} &= 0.237088(46) - 0.1008(34)N_f \end{aligned} \tag{33}$$

where the quenched ($N_f = 0$) results are taken from Ref. [12] and we have propagated the errors by quadrature into $c_0^{(1)}$.

A. Effect on gauge action couplings

The MILC and UKQCD Collaborations use a "tadpole improved" version of Eqn. (11), dividing each gauge link by a factor u_0. In addition, a factor of c_0/u_0^4 is subsumed into the gauge coupling $\beta_0 = 6c_0/(g^2u_0^4)$ that multiplies the plaquette term P_0 [15]. The couplings multiplying the "planar rectangles" P_1 and "parallelograms" P_2 are [6, 15]

$$\begin{aligned} \beta_1 &= -\frac{\beta_0}{20u_0^2}\left[1 - \left(\frac{12\pi}{5}c_0^{(1)} + 48\pi c_1^{(1)} + 2u_0^{(1)}\right)\alpha_s\right] , \\ \beta_2 &= \frac{12\pi\beta_0}{5u_0^2}c_2^{(1)}\alpha_s , \end{aligned} \tag{34}$$

(with factors of 4π coming from converting from g^2 to α_s). The quenched radiative contributions have been analyzed in [15] and so we may write

$$\begin{aligned} \beta_1 &= -\frac{\beta_0}{20u_0^2}\left[1 + 0.4805\alpha_s - \left(\frac{12\pi}{5}c_{0,f}^{(1)} + 48\pi c_{1,f}^{(1)}\right)\alpha_s\right] , \\ \beta_2 &= -\frac{\beta_0}{u_0^2}\left(0.033\alpha_s - \frac{12\pi}{5}c_{2,f}^{(1)}\alpha_s\right) , \end{aligned} \tag{35}$$

where now all the one-loop coefficients $c_{i,f}^{(1)}$ contain only quark loop contributions.

Plugging in the numbers for the HISQ action obtained in this work we find

$$\begin{aligned} \beta_1 &= -\frac{\beta_0}{20u_0^2}\left[1 + 0.4805\alpha_s - 0.899(52)N_f\alpha_s\right] , \\ \beta_2 &= -\frac{\beta_0}{u_0^2}\left[0.033\alpha_s - 0.0121(23)N_f\alpha_s\right] . \end{aligned} \tag{36}$$

The full coefficient c_0 has here been absorbed into the gauge coupling, so the coefficient multiplying the plaquette P_0 is simply $\beta_p = \beta_0$. For the HISQ action, the fermionic contribution to c_0 (i.e. $c_{0,f}^{(1)}$ in Eqn. (33)) is large and sizeable shifts will be needed in β_0 to maintain a constant g^2 (or lattice spacing) as N_f is changed from 0 (quenched) to $N_f = 3$ or 4. Whilst this is not a problem in itself, it does make it more difficult to intuitively relate values of β_0 to the lattice spacing.

A more sensible choice is to absorb just the tree-level portion $c_0^{(0)} = \frac{5}{3}$ into the gauge coupling. The overall gauge coupling is simply $\beta_0' = 10/(g^2u_0^4)$. Using primes to denote couplings in this scheme, the coupling multiplying the plaquette in the action is now

$$\begin{aligned} \beta_p' &= \beta_0'\left[1 + \frac{4\pi c_0^{(1)}}{c_0^{(0)}}\alpha_s\right] \\ &= \beta_0'\left[1 + 1.7876\alpha_s - 0.760(26)N_f\alpha_s\right] . \end{aligned} \tag{37}$$

The remaining couplings in this scheme are

$$\begin{aligned} \beta_1' &= -\frac{\beta_0'}{20u_0^2}\left[1 - \left(48\pi c_1^{(1)} + 2u_0^{(1)}\right)\alpha_s\right] \\ &= -\frac{\beta_0'}{20u_0^2}\left[1 + 2.2681\alpha_s - \left(48\pi c_{1,f}^{(1)}\right)\alpha_s\right] \\ &= -\frac{\beta_0'}{20u_0^2}\left[1 + 2.2681\alpha_s - 1.659(46)N_f\alpha_s\right] , \\ \beta_2' &= \frac{12\pi\beta_0'}{5u_0^2}c_2^{(1)}\alpha_s \\ &= -\frac{\beta_0'}{u_0^2}\left[0.033\alpha_s - 0.0121(23)N_f\alpha_s\right] . \end{aligned} \tag{38}$$

The factors multiplying the gauge coupling in β_2 and β_2' are the same as this term is already $\mathcal{O}(\alpha_s)$.

IV. RADIATIVE IMPROVEMENT AND THE STATIC POTENTIAL

In this section, we seek to understand what effect the omission of the asqtad $\mathcal{O}(N_f\alpha_s a^2)$ corrections to gauge action will have on physical observables measured in existing non-perturbative Monte Carlo lattice simulations.

As discussed above, the then-unknown $\mathcal{O}(N_f\alpha_s a^2)$ contributions to c_i were omitted from the current generation of three-flavour dynamical asqtad simulations. Perturbatively, this omission will lead to an imperfect cancellation of discretisation effects and a residual breaking of rotational symmetry in the static quark potential. Similar effects are expected to be seen in the numerical simulation results, and hence in the determinations of the scale-setting parameters $\hat{r}_1$, $\hat{r}_0$ derived from the static potential.

Here we use one-loop perturbation theory to calculate the effect of the missing $\mathcal{O}(N_f\alpha_s a^2)$ terms on the static potential and particularly on the scale-setting parameters

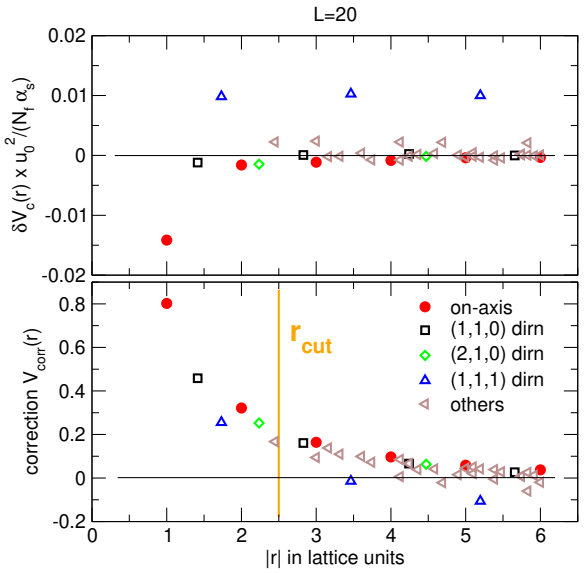

FIG. 4: The perturbative correction (top panel) and the correction for lack of rotational invariance (bottom panel).

$\hat{r}_1$, $\hat{r}_0$. The rationale for this and alternative approaches are discussed in Secs. I and V.

A. The correction to the static potential

Including the missing $\mathcal{O}(N_f\alpha_s a^2)$ corrections to the gauge action would change the lattice static-quark potential $V(\mathbf{r})$ measured by the MILC Collaboration by an amount $\delta V(\mathbf{r})$. Here we estimate this change using one-loop perturbation theory.

We do this by computing the spatial Fourier transform (for zero temporal momentum) of $G_{0\mu}(k)\Delta_{\mu\nu}(k)G_{\nu 0}(k)$, where $G_{\mu\nu}(k)$ is the tree-level Symanzik improved gluon propagator at momentum $k = (0, \mathbf{k})$, as shown in Fig. 3. $\Delta_{\mu\nu}(k)$ is the $\mathcal{O}(g^2)$ insertion into the gluon propagator arising from the perturbative expansion of the $\mathcal{O}(N_f\alpha_s a^2)$ corrections to the gauge action in Eqn. (11) with appropriate asqtad $c^{(1)}_{i,f}$ couplings [6]. Again, Feynman rules are derived using the HiPPy package [19, 20].

In all cases, the spatial Fourier transforms are carried out for a finite, periodic lattice of spatial volume L^3.

The gauge action has $c_3 = 0$, but the static quark counterterm proportional to c_4 is also omitted. This will also affect the success of the radiative improvement, but we do not consider its effect in this paper.

The result for $L = 20$ is shown in the upper panel of Fig. 4. We expect the *corrected* lattice potential to be rotationally symmetric at $\mathcal{O}(\alpha_s a^2)$, so the lack of rotational invariance in the upper panel of Fig. 4 is indicative of an equal and opposite breaking of rotational symmetry in the potential measured on ensembles that omit the $\mathcal{O}(N_f\alpha_s a^2)$ radiative corrections.

B. The effect of the correction

To set the scale, the MILC Collaboration measure the static potential for a variety of on- and off-axis spatial separations: $\{V(\mathbf{r}_i)\}$ with associated statistical errors $\{\sigma(\mathbf{r}_i)\}$. A least squares fit is performed using the fit function [31, 32, 33]

$$
\begin{aligned}
V_{\rm fit}(\mathbf{r}) &= V_{\rm cont}(r) + b_3 V_{\rm corr}(\mathbf{r}) \equiv \sum_{j=0}^{3} b_j f_j(\mathbf{r}) \ , \\
V_{\rm cont}(r) &= b_0 - \frac{b_1}{r} + b_2\, r \ , \\
V_{\rm corr}(\mathbf{r}) &= \begin{cases} V_{\rm free}(\mathbf{r}) - \frac{1}{r} & r < r_{\rm cut} \\ 0 & \text{otherwise} \end{cases}
\end{aligned}
$$

which defines basis functions $f_j(\mathbf{r})$ with a vector of fit parameters $\underline{b}$. $V_{\rm corr}$ aims to account for the lack of rotational invariance at small $r \equiv |\mathbf{r}|$, with $V_{\rm free}$ the finite-sized lattice estimate for $1/r$ from the Fourier transform of the (free) Symanzik gluon Coulomb propagator. We show this for $L = 20$ in the lower panel of Fig. 4.

In more detail, the fit minimises the least-squared function

$$
L(\underline{b}) = \sum_i \frac{\left(V(\mathbf{r}_i) - V_{\rm fit}(\mathbf{r}_i)\right)^2}{\sigma(\mathbf{r}_i)^2} \ . \tag{39}
$$

We define the (weighted) average of operator $A(\mathbf{r})$ over a set of measured $\mathbf{r}_i$ as

$$
\langle A \rangle = \sum_i^N \frac{A(\mathbf{r}_i)}{\sigma(\mathbf{r}_i)^2} \Bigg/ \sum_i^N \frac{1}{\sigma(\mathbf{r}_i)^2} \ . \tag{40}
$$

The result of the least squares fitting is a vector of best-fit parameters $\underline{b}$ that obeys the linear equation

$$
M_{jk}\, b_k = X_j \quad \Rightarrow \quad \underline{b} = M^{-1}\underline{X} \tag{41}
$$

where

$$
M_{jk} = \langle f_j f_k \rangle \ , \quad X_j = \langle f_j V \rangle \ . \tag{42}
$$

Having done this, the lattice scale is set from the analytic derivative of the $V_{\rm cont}(r)$ function:

$$
\hat{r}_n^2 \frac{dV_{\rm cont}(r)}{dr}\bigg|_{\hat{r}_n} = C_n \quad \Rightarrow \quad \hat{r}_n = \sqrt{\frac{C_n - b_1}{b_2}} \ . \tag{43}
$$

We use "hats" here to stress that the scale parameters are measured in dimensionless lattice units.

Two scales are commonly used: $\hat{r}_1$ from $C_1 = 1$ (physical value $r_1 = 0.317$ fm [33]) and $\hat{r}_0$ from $C_0 = 1.65$ (physical value $r_0 = 0.462$ fm [33]). In general $\hat{r}_1$ is preferred as the statistical errors on the static potential are smaller at shorter distances.

C. The corrected fits

Having calculated the $\mathcal{O}(N_f\alpha_s a^2)$ corrections to the static potential, we can now calculate the effect of including δV on the best fit parameters b_j, assuming that we carry out exactly the same fitting procedure as before.

We would now minimise

$$L'(\underline{b}) = \sum_i \frac{\left(V(\mathbf{r}_i) + \alpha_s \delta V(\mathbf{r}_i) - V_{\rm fit}(\mathbf{r}_i)\right)^2}{\sigma(\mathbf{r}_i)^2} \ . \qquad (44)$$

Given that $\underline{b}$ minimises $L(\underline{b})$, we assert that $\underline{b}' = \underline{b} + \alpha_s \delta\underline{b}$ minimises $L'(\underline{b})$, with

$$\delta\underline{b} = M^{-1}\delta\underline{X} \qquad (45)$$

and $\delta X_j = \langle f_j \ \delta V\rangle$.

After finding $\delta\underline{b}$ we can deduce the associated change in $\hat{r}_1$. We can either define this as $\delta\hat{r}_1 = \hat{r}_1(\underline{b}+\alpha_s\delta\underline{b}) - \hat{r}_1(\underline{b})$ or, using a Taylor expansion of Eqn. (43),

$$\frac{\delta\hat{r}_1}{\hat{r}_1} = -\frac{1}{2}\left(\frac{\delta b_1}{1-b_1} + \frac{\delta b_2}{b_2}\right) \ . \qquad (46)$$

The two methods give almost identical results.

D. Results

We looked at a range of ensembles listed in Table I, using published values of u_0 to infer the strong coupling constant in the same way as MILC [34]:

$$\alpha_s = -\frac{4\log u_0}{3.0684} \ . \qquad (47)$$

To estimate the effect the fermionic corrections would have on the scale setting parameters as measured by the MILC Collaboration, we adopt the same fitting function and we use the same fit range $\sqrt{5} \le r \le 7$ and $r_{\rm cut} = 3$ for the "fine" lattices and $\sqrt{2} \le r \le 6$ with $r_{\rm cut} = 2.5$ for the "coarse" and "very coarse" ensembles.

We infer b_1 and b_2 from published values for $\hat{r}_1$ and $\hat{r}_0$ on given ensembles [32, 35]:

$$b_2 = \frac{1.65 - 1}{\hat{r}_0^2 - \hat{r}_1^2}, \quad b_1 = 1 - b_2\ \hat{r}_1^2 \ . \qquad (48)$$

For instance, on the $\beta = 6.76$, $m_u/m_s = 0.01/0.05$ coarse ensemble $\hat{r}_1 = 2.60$ (Ref. [32]), $\hat{r}_0 = 3.76$ (Ref. [35]) giving $b_1 = 0.406$, $b_2 = 0.088$. We then find

$$\delta\hat{r}_1/\hat{r}_1 = -0.65\%, \quad \delta\hat{r}_0/\hat{r}_0 = -0.11\%. \qquad (49)$$

The shift in $\hat{r}_1$ is larger because $\hat{r}_1$ is smaller than $\hat{r}_0$ and δV is short-ranged. On the fine lattices, $\hat{r}_1$ in lattice units is comparable to $\hat{r}_0$ on the coarse lattices. The shift is therefore small. Results for other ensembles are given in Table I

We have looked at various scenarios, e.g. different choices for the fitted range of $\{\mathbf{r}_i\}$ and constraining some fit parameters to zero. Whilst the precise shifts do vary, the scale (and sign) of the shifts remain stable under such variations.

V. DISCUSSION

Radiatively improved gluon actions are used in lattice simulations to give greater control over discretisation effects and to reduce the uncertainty in continuum-extrapolated quantities. A typical example is the use of the Lüscher-Weisz action in improved staggered simulations by the MILC and UKQCD Collaborations.

We note that current unquenched simulations employing lattice quark formulations other than improved staggered, such as domain wall or improved Wilson clover, generally do not use a radiatively improved action for the gluons; hence a calculation of the effects of fermion loops on the gluonic action is currently neither necessary nor useful for those simulations, but could readily be performed if and when simulations using such quark actions together with the Lüscher-Weisz action will be undertaken.

Simulations employing staggered quarks rely on the validity of the "fourth root trick", which has not yet been rigorously established. The purpose of this paper is not to engage in the debate about the validity of this procedure, but merely point out that simulations using improved staggered quarks have produced results in excellent agreement with experiment so far. While we cannot completely discard the possibility that the observed scaling violation in Φ_B might be an indication of some more fundamental problem, we believe that our explanation for this scaling violation is more likely in the light of existing evidence. In particular, we are able to replicate both the sign and the rough magnitude of the observed effect by a perturbative calculation.

The shift in the radiative corrections due to the HISQ fermions in Eqns. (33,36) is surprisingly large, even compared to the coefficients for asqtad fermions [6]. At first sight, this may seem like a surprise, since HISQ is supposed to be the more highly-improved action. However, HISQ is designed to suppress taste-changing interactions coming from low momentum quark/high momentum gluon couplings, but the gluonic improvement coefficients come from high momentum quark/low momentum gluon couplings, for whose suppression the HISQ action is not tuned.

One consequence is that if the coefficient c_0 is subsumed into the leading factor of β_0, we expect to see large N_f dependent shifts in the value of β_0 at fixed g^2, and we also give results for an alternate scheme where only the tree level part of c_0 is included in the overall gauge coupling.

The radiative corrections in the Lüscher-Weisz action used by MILC in the asqtad simulations, however, omit the contribution from dynamical sea quarks. This contribution has recently been calculated at one-loop for N_f (massless) flavours of asqtad improved staggered fermions. The results are dramatic, leading to sign reversals in some of the radiative coefficients.

It is therefore conceivable that the omission of the $\mathcal{O}(N_f\alpha_s a^2)$ corrections leads to increased scaling viola-

TABLE I: MILC simulation parameters and shifts in scale setting parameters induced by *omission* of fermionic radiative corrections to the gluonic action. Smoothed $\hat{r}_1$ values are from Ref. [33, 36]. $\hat{r}_0$ values are then inferred from the ratios $\hat{r}_0/\hat{r}_1$ given in Ref. [33]. We have estimated u_0 for the very coarse ensemble. Lattice spacings are quoted as approximate guides; precise values may be inferred from setting $r_1 = 0.317$ fm.

Label	a/fm (approx)	$L^3 \times T$	Sea quark masses m_l/m_s	$\hat{r}_1$	$\hat{r}_0$	u_0	$\delta\hat{r}_1/\hat{r}_1$ (in %)	$\delta\hat{r}_0/\hat{r}_0$ (in %)
very coarse	0.18	$16^3 \times 48$	0.082/0.082	1.805 (10)	2.622 (28)	0.8585	−1.11	−0.40
coarse	0.12	$20^3 \times 64$	0.02/0.05	2.650 (8)	3.828 (15)	0.8688	−0.63	−0.11
			0.01/0.05	2.610 (12)	3.774 (20)	0.8677	−0.65	−0.11
		$24^3 \times 64$	0.005/0.05	2.632 (13)	3.834 (25)	0.8678	−0.64	−0.10
fine	0.09	$28^3 \times 96$	0.0124/0.031	3.711 (13)	5.398 (28)	0.8788	0.01	0.00
			0.0062/0.031	3.684 (12)	5.384 (27)	0.8782	0.01	0.00

tions in results from dynamical simulations when compared to quenched data.

To properly establish whether this is the case would require a new set of dynamical Monte Carlo simulations, which is well beyond the scope of this study. An alternative is to attempt a reweighting of the existing ensembles using factors $e^{-\delta S}$ based on the $\mathcal{O}(N_f\alpha_s a^2)$ counterterms. Such calculations notoriously suffer from a very poor overlap between the importance samplings of the original and reweighted ensembles for even minor changes in the action. This leads to very large statistical errors which will obscure any sought-for effect.

We have therefore used instead one-loop lattice perturbation theory to estimate the effect of the $\mathcal{O}(N_f\alpha_s a^2)$ corrections on the static potential and the shifts in the scale-setting parameters $\hat{r}_1$ and $\hat{r}_0$ arising from the *omission* of the fermionic radiative corrections for typical values of the simulations with $2+1$ dynamical asqtad flavours.

On *fine* ($a \simeq 0.09$ fm) lattices, the shifts in $\hat{r}_1$ and $\hat{r}_0$ are negligible (less than 0.1%) and will be at least as small on *superfine* lattices with $a \simeq 0.06$ fm. On *coarse* lattices ($a \simeq 0.12$ fm), omission of the corrections leads to $\hat{r}_1$ being 0.6% too large, with $\hat{r}_0$ unaffected. On *very coarse* lattices ($a \simeq 0.18$ fm), $\hat{r}_1$ is 1.1% too large and $\hat{r}_0$ 0.4% too large.

Overall, then, the omission of the $\mathcal{O}(N_f\alpha_s a^2)$ leads to an underestimate of the lattice spacing on coarser lattices as defined using $\hat{r}_1$. Whilst numerically small, this effect is comparable to the statistical errors on a number of quantities and therefore would lead to a measurable increase in the statistical uncertainty of continuum-extrapolated lattice QCD predictions.

Higher loop and non-perturbative effects will almost certainly change the exact value of the shift in $\hat{r}_1$, but are unlikely to alter our main conclusion: that the effect is measurable.

Putting aside the static potential, an alternative approach to fixing the lattice spacing is to use the $2S-1S$ mass splitting of Υ states. We have seen that that the correction $\delta V(\mathbf{r})$ is negative, so including the $\mathcal{O}(N_f\alpha_s a^2)$ radiative corrections would decrease slightly both (lattice) Υ masses. Because $\delta V(\mathbf{r})$ is short-ranged, the effect on the $1S$ state will be larger than on the $2S$ state since the $1S$ wavefunction is larger at small r. The lattice mass splitting and thus the derived value of a will increase, and thus Φ_B will get slightly smaller in such physical units on coarse lattices. To reliably deduce this fact from the Υ mass gap, however, we need to include the effect of the contact term, Eqn. (3), which we do not yet know.

Acknowledgments

We thank C.T.H. Davies, U.M. Heller, G.P. Lepage and D. Toussaint for useful conversations and comments. A.H. thanks the U.K. Royal Society for financial support. G.M.v.H. was supported by the Deutsche Forschungsgemeinschaft in the SFB/TR 09. This work has made use of the resources provided by: the Darwin Supercomputer of the University of Cambridge High Performance Computing Service (`http://www.hpc.cam.ac.uk`), provided by Dell Inc. using Strategic Research Infrastructure Funding from the Higher Education Funding Council for England; the Edinburgh Compute and Data Facility (`http://www.ecdf.ed.ac.uk`), which is partially supported by the eDIKT initiative (`http://www.edikt.org.uk`); the Fermilab Lattice Gauge Theory Computational Facility. The University of Edinburgh is supported in part by the Scottish Universities Physics Alliance (SUPA).

[1] HPQCD, C. T. H. Davies *et al.*, Phys. Rev. Lett. **92**, 022001 (2004), [hep-lat/0304004].

[2] MILC, K. Orginos, D. Toussaint and R. L. Sugar, Phys. Rev. **D60**, 054503 (1999), [hep-lat/9903032].

[3] HPQCD, E. Follana *et al.*, Phys. Rev. **D75**, 054502 (2007), [hep-lat/0610092].

[4] K. Y. Wong and R. M. Woloshyn, PoS **LAT2007**, 047 (2007), [0710.0737].

[5] MILC, A. Bazavov *et al.*, PoS **LAT2008**, 033 (2008), [0903.0874].

[6] Z. Hao, G. M. von Hippel, R. R. Horgan, Q. J. Mason and H. D. Trottier, Phys. Rev. **D76**, 034507 (2007), [0705.4660].

[7] A. Hart, G. M. von Hippel and R. R. Horgan, PoS **LAT2008**, 046 (2008), [0808.1791].

[8] UKQCD, E. B. Gregory, A. C. Irving, C. McNeile and C. M. Richards, 0810.0136.

[9] HPQCD, A. Gray *et al.*, Phys. Rev. Lett. **95**, 212001 (2005), [hep-lat/0507015].

[10] C. Davies, private communication.

[11] P. Weisz and R. Wohlert, Nucl. Phys. B **236**, 397 (1984).

[12] J. R. Snippe, Nucl. Phys. **B498**, 347 (1997), [hep-lat/9701002].

[13] M. Lüscher and P. Weisz, Phys. Lett. **B158**, 250 (1985).

[14] P. Weisz, Nucl. Phys. B **212**, 1 (1983).

[15] M. G. Alford, W. Dimm, G. P. Lepage, G. Hockney and P. B. Mackenzie, Phys. Lett. **B361**, 87 (1995), [hep-lat/9507010].

[16] G. P. Lepage, hep-lat/9607076.

[17] M. Lüscher and P. Weisz, Nucl. Phys. **B266**, 309 (1986).

[18] M. Lüscher and P. Weisz, Commun. Math. Phys. **97**, 59 (1985).

[19] A. Hart, G. M. von Hippel, R. R. Horgan and L. C. Storoni, J. Comput. Phys. **209**, 340 (2005), [hep-lat/0411026].

[20] A. Hart, G. M. von Hippel and R. R. Horgan, Comput. Phys. Commun., in preparation.

[21] I. T. Drummond, A. Hart, R. R. Horgan and L. C. Storoni, Nucl. Phys. Proc. Suppl. **119**, 470 (2003), [hep-lat/0209130].

[22] M. A. Nobes, H. D. Trottier, G. P. Lepage and Q. Mason, Nucl. Phys. Proc. Suppl. **106**, 838 (2002), [hep-lat/0110051].

[23] M. A. Nobes and H. D. Trottier, Nucl. Phys. Proc. Suppl. **129**, 355 (2004), [hep-lat/0309086].

[24] H. D. Trottier, Nucl. Phys. Proc. Suppl. **129**, 142 (2004), [hep-lat/0310044].

[25] G. 't Hooft, Nucl. Phys. **B153**, 141 (1979).

[26] G. Parisi, Invited talk given at Summer Inst. Progress in Gauge Field Theory, Cargese, France, Sep 1-15, 1983.

[27] D. H. Adams and W. Lee, Phys. Rev. D **77** 045010 (2008), [0709.0781].

[28] K. Symanzik, Nucl. Phys. **B226**, 187 (1983).

[29] G. M. von Hippel, Comput. Phys. Commun. **174**, 569 (2006), [physics/0506222].

[30] G. M. von Hippel, arXiv:0704.0274.

[31] C. W. Bernard *et al.*, Phys. Rev. **D62**, 034503 (2000), [hep-lat/0002028].

[32] C. W. Bernard *et al.*, Phys. Rev. **D64**, 054506 (2001), [hep-lat/0104002].

[33] C. Aubin *et al.*, Phys. Rev. **D70**, 094505 (2004), [hep-lat/0402030].

[34] MILC, K. Orginos and D. Toussaint, Phys. Rev. **D59**, 014501 (1999), [hep-lat/9805009].

[35] D. Toussaint, private communication.

[36] HPQCD, E. Follana, C. T. H. Davies, G. P. Lepage and J. Shigemitsu, Phys. Rev. Lett. **100**, 062002 (2008), [0706.1726].

[37] Of course, this introduces higher dimensional operators into the theory, both from the field redefinition and from the Jacobian, but such operators are irrelevant from the point of view of the renormalisation group [15, 16]. Alternatively, by introducing such operators in the original theory, we can arrange for their coefficients to vanish after the redefinition.

[38] We note in passing here that an alternative to the above procedure, we could instead choose to remove the static quark counterterm from the outset by using the equations of motion to set $c_4 = 0$. We would then, however, have to include a non-zero c_3 to counter the effect of a_3 leading to the inclusion of all three improvement terms in the gauge action.